

# **1     Dynamical Model of Drug Accumulation in Bacteria: Sensitivity Analysis and** **2     Experimentally Testable Predictions**

3

4     Neda Vesselinova<sup>1,2</sup>, Boian S. Alexandrov<sup>1</sup>, and Michael E. Wall<sup>\*3</sup>

5

6     <sup>1</sup>Theoretical Division, Los Alamos National Laboratory, Los Alamos NM 87545

7     <sup>2</sup>University of California, Los Angeles, CA 90095

8     <sup>3</sup>Computer, Computational, and Statistical Sciences Division, Los Alamos National  
9     Laboratory, Los Alamos NM 87545

10

11     \*Corresponding author

12

13     November 4, 2015

14

15     LA-UR-15-28626

**Abstract.** We present a dynamical model of drug accumulation in bacteria. The model captures key features in experimental time courses on ofloxacin accumulation: initial uptake; short-term response; and long-term adaptation. In combination with experimental data, the model provides estimates of import and export rates in each phase, the latency in the short-term response, and the rate of increase in efflux during adaptation. Global sensitivity analysis, local sensitivity analysis, and Bayesian sensitivity analysis of the model provide information about the robustness of these estimates, and about the relative importance of different features of the accumulation time courses in three different bacterial species: *Escherichia coli*, *Staphylococcus aureus*, and *Pseudomonas aeruginosa*. The results lead to experimentally testable predictions of membrane permeability and drug efflux and trapping, which influence drug resistance. A key prediction is that an increase in *E. coli* ofloxacin accumulation is accompanied by a decrease in membrane permeability, suggesting that, depending on changes in other factors, decreasing permeability is not always an effective drug resistance strategy.

**Author Summary.** Bacteria live or die depending on how much antibiotic gets inside them. Using a simple mathematical model, detailed information about drug import and export can be teased out of time courses of internal drug levels after a sudden environmental exposure. The results reveal that blocking diffusion across the membrane is not always an effective drug resistance strategy for bacteria.

# Introduction

Drug resistance in bacteria can be increased by efflux pump systems [1], and pump inhibition has emerged as a strategy for overcoming drug resistance [2]. Many details of how efflux pumps work are still unclear, however. In particular, quantitative information about how efflux influences drug accumulation in bacteria is still scarce [3].

Drug accumulation is a key factor in obtaining a quantitative understanding of resistance. For example, predictions of minimum inhibitory concentrations (MICs) of  $\beta$ -lactams in *Escherichia coli* were obtained by equating the steady state periplasmic drug concentration with a periplasmic binding protein inhibitory concentration [4]. A predicted MIC was calculated as the *external* concentration that would yield the accumulated *internal* inhibitory concentration in steady state, considering flux terms from membrane permeation and  $\beta$ -lactamase degradation. MIC predictions also have been made considering the action of efflux pumps on cephalosporins [5] and  $\beta$ -lactams [6] in *E. coli*. These predictions were accompanied by estimates of efflux pump Michaelis-Menten kinetic constants (*i.e.*,  $K_m$  and  $k_{cat}$  values), providing an explicit connection between efflux and resistance.

Time-dependent drug accumulation studies also have yielded insight into drug transport [7-9]. Diver et al. [8] found exposure of *E. coli* to five different quinolones induced a rapid  $\sim 10$  sec uptake followed by a  $\sim 30$  min phase of more gradual

accumulation. Similar two phase behavior was seen by Asuquo and Piddock [7] in accumulation of fifteen different quinolones in *E. coli*, *Pseudomonas aeruginosa*, and *Staphylococcus aureus* [7]. Whereas drug levels appeared to plateau in *E. coli* and *S. aureus*, levels in *P. aeruginosa* gradually decreased at longer times, suggesting an adaptation process [7].

Mathematical modeling has provided substantial insights into accumulation of beta-lactams [4,6], cephalosporins [5], and tetracycline [9] in *E. coli*. Quinolone accumulation, however, has not yet been analyzed in the context of a mathematical model. Here we present a mathematical model of drug accumulation and use it to analyze experimental data on accumulation of the quinolone oxfloracin in *E. coli*, *S. aureus*, and *P. aeruginosa* [7]. The analysis yields estimates of permeation and efflux rates, the latency in the short-term response, and the rate of increase in efflux during adaptation. We also perform global sensitivity analysis, local sensitivity analysis, and Bayesian sensitivity analysis of the model. The sensitivity analyses provide information about the robustness of parameter estimates and enable assessment of the relative importance of the short-term response and long-term adaptation in different bacterial species.

The results lead to experimentally testable predictions of membrane permeability and drug efflux and trapping, which influence drug resistance. A key prediction is that an increase in *E. coli* drug accumulation is accompanied by a decrease in membrane permeability, illustrating that decreasing permeability, although

commonly associated with increased drug resistance [10], is not always an effective drug resistance strategy for bacteria. Overall the results indicate the utility of mathematical modeling and sensitivity analysis in obtaining new insights into drug accumulation in bacteria.

## Results

### *Model behavior*

Our model of drug accumulation (Methods) was designed to describe two phases of drug accumulation dynamics, with long-term adaptation in the second phase (Fig. 1). After exposure at  $t = 0$ , the first phase begins, where cellular antibiotic levels rise and relax toward an asymptotic value  $a_1$ . The relaxation in this phase is exponential with rate  $\beta_1$ . At time  $t = \tau$ , the second phase begins, where antibiotic levels may either rise or fall towards a new asymptotic value  $a_2$ . The relaxation in this phase is initially dominated by exponential relaxation with rate  $\beta_2$ . Later, adaptation can dominate the dynamics, following  $[1 + \delta(t - \tau)]^{-1}$ . Together these features capture the full set of behaviors exhibited by the experimental data on ofloxacin accumulation [7] (Fig. 2).

### *Parameter estimates*

Parameter values were estimated by fitting the model to data on ofloxacin accumulation in *E. coli*, *P. aeruginosa*, and *S. aureus*. Following Ref. [7], the fits were performed assuming a uniform measurement error. (Rough error estimates for the data, inferred from the values given for the norfloxacin, are: 4.6 ng/mg for *E. coli*; 1.5 ng/mg for *P. aeruginosa*; and 8.7 ng/mg for *S. aureus*.) Reasonable fits were obtained for all datasets (Fig. 2). Parameter values varied substantially for different bacteria (Table 1), as expected given the differing behaviors. *E. coli* exhibits two phases of accumulation with little apparent long-term adaptation, consistent with the low value of  $\delta$ . *P. aeruginosa* shows a stronger adaptation response, corresponding to the higher value of  $\delta$ . *S. aureus* exhibits a single phase response without adaptation, consistent with the value of  $\tau$  being greater than the longest time point.

## ***Sensitivity analysis results***

Sensitivity analysis is a technique for evaluating how variations in the output of a mathematical model are related to variations in the model inputs. We used sensitivity analysis to assess the importance of different model parameters in determining the antibiotic accumulation behavior. We performed three independent analyses using: global sensitivity analysis (GSA), local sensitivity analysis (LSA), and Bayesian sensitivity analysis (BSA). For each analysis, the time courses using the optimal parameter values were used as reference behaviors.

*Global sensitivity analysis.* GSA explores the sensitivity of the model output within the entire (prior) parameter space of the model inputs. We performed variance-based GSA [11], which decomposes the variance of the output into parts ascribed to different input parameters using a Fourier Haar decomposition [12,13]. Both the “total effect” and “main effect” for each input parameter were calculated using the Sobol Monte Carlo algorithm [14]; here we focus on the total effect results. The prior range of the input parameters was defined using uniform logarithmic distributions given in Table 2.

GSA results for *E. coli*, *P. aeruginosa*, and *S. aureus* are shown in Figure 3. For *E. coli*,  $\beta_1$  exerts the highest total effect initially, followed by  $a_1$ ,  $\tau$ , and  $a_2$ . The effect of  $\beta_2$  never dominates, but is substantial at early times. The sensitivity to  $\delta$  is low at all times. For *P. aeruginosa*,  $a_1$  exerts the highest total effect initially, followed by  $\tau$  and  $a_2$ . In contrast with *E. coli*, the sensitivity to  $\delta$  is high for *P. aeruginosa*, while both  $\beta_1$  and  $\beta_2$  show low sensitivity. For *S. aureus*,  $\beta_1$  exerts the highest total effect early on, shifting to  $a_1$  and then  $\tau$  at later times. The effects of  $a_2$  and  $\beta_2$  are smaller by comparison. Like for *E. coli*, the sensitivity to  $\delta$  is low.

*Local sensitivity analysis.* LSA has a rich history of use in assessing the robustness of biochemical network model behavior to changes in parameter values [15,16]. In LSA, the local gradients of the model output are calculated with respect to model parameters at a fixed point. Here we use the gradients to define a covariance matrix of variations [17] (Methods), and interpret the LSA in terms of the eigenvalues and

eigenvectors of the covariance matrix. Small eigenvalues are associated with parameter combinations that show higher sensitivity.

We performed LSA on the *P. aeruginosa* model, for comparison to the GSA. Each eigenvector in the LSA is strongly associated with a single parameter (Fig. 4a), facilitating the interpretation. The three smallest eigenvalues (Fig. 4b) are those associated with  $a_1$ ,  $a_2$ , and  $\delta$  (corresponding to eigenvectors 1-3 in Fig. 4a), indicating that the sensitivity of the model to these parameters is relatively high. The parameters  $\beta_1$ ,  $\beta_2$  and  $\tau$  are associated with orders of magnitude higher eigenvalues, indicating that the sensitivity to these parameters is relatively low.

*Bayesian sensitivity analysis.* BSA estimates the probability density functions (pdf's) of the model parameters given observed data and measurement errors using Bayes' theorem [18,19]. Like GSA, BSA requires prior distributions of the model inputs. The more sensitive is the model parameter, the more constrained is the posterior pdf compared to the prior pdf.

Figure 5 shows Bayesian sensitivity analysis for the *P. aeruginosa* model. Here, the Bayesian analysis identifies a Markov-Chain Monte Carlo (MCMC) sample of models that are consistent with the observed data, assuming a uniform measurement error [7]. The histograms along the diagonal represent the posterior pdf's of the model parameters constrained by the model observations. Each dot in the off-diagonal scatter plots represents a model-parameter set from the final MCMC sample. Some of the parameters,



$a_1$ ,  $a_2$ , and  $\delta$  appear to have peaked distributions, indicating a sharpened sensitivity within the posterior range. The probability density of  $\tau$  is uniform at longer times and zero at shorter times. The distributions of  $\beta_1$  and  $\beta_2$  are flat, and, therefore they are less sensitive parameters. The scatter plot between  $a_2$  and  $\delta$  is extended along the  $a_2$ - $\delta$  direction, indicating that these parameters are correlated.

### ***Experimentally testable predictions of permeability and efflux***

We used Eqs. (5) and (6) to predict permeability and efflux given the estimated parameters. The predictions are quantified in the form of the efflux rate,  $\varepsilon(t)$ , which is defined as the portion of the specific export rate not associated with permeation, and the accumulation factor,  $\phi(t)$ , which is defined as  $\alpha(t)/\beta(t)$ , the ratio of the permeability to the export rate. Depending on the sign of  $\varepsilon(t)$ , qualitatively different mechanisms are at work: a positive value is associated with efflux, while a negative value is associated with trapping.

The resulting predictions of  $\varepsilon(t)$  and  $\phi(t)$  are shown in Table 4. The robustness of these predictions depends on the robustness of the estimation of  $a_1$  and  $\beta_1$ , for  $t < \tau$ , and  $a_2$  and  $\beta_2$ , for  $t = \tau$ . According to the sensitivity analysis, the estimates of some of these parameters are not robust, yielding unreliable predictions for some of the *P. aeruginosa* and *S. aureus* values. For completeness, the unreliable predictions are listed in Table 4, but are enclosed in parentheses.

### **Discussion**

## ***Interpretation of sensitivity analysis results***

*Global Sensitivity Analysis:* Results obtained using the GSA suggest that the relative importance of the various model parameters in determining the output behavior of the simulations differs for *E. coli*, *P. aeruginosa*, and *S. aureus* (Figure 3). However, there are also some similarities. In most cases,  $a_1$  and  $\beta_1$  are important only at very early-times right at the beginning of the data collection. This suggests that proper estimation of  $a_1$  and  $\beta_1$  requires accurate early-time measurements. In all cases, the sensitivity of  $a_1$  and  $\beta_1$  diminishes over time. Also in all cases, the sensitivity of  $a_1$  increases with time. The temporal behavior of  $\beta_2$  sensitivity is very different in all three cases:  $\beta_2$  is relatively important at early times for the case of *E. coli*;  $\beta_2$  is unimportant for the case of *P. aeruginosa*; and the  $\beta_2$  sensitivity peaks at the mid-times for the case of *S. aureus*. Interestingly, the parameter  $\delta$  is important only for the case of *P. aeruginosa*. The temporal behavior of  $\tau$  sensitivity is similar for the case of *E. coli* and *P. aeruginosa* ( $\tau$  sensitivity is decreasing with time), but very different for the case of *S. aureus* ( $\tau$  sensitivity is increasing with time).

*Local sensitivity analysis:* The global and local sensitivity analyses yield similar results for *P. aeruginosa*. Both analyses identify  $a_1$ ,  $a_2$ , and  $\delta$  as sensitive model parameters. However, the global and local sensitivity analyses produce different sensitivity estimates related to the parameter  $\tau$ . The model is sensitive to this

parameter according to GSA but not according to LSA. This suggests that when all the model parameters are at their optimal values, small deviations in  $\tau$  values have a small impact on the optimal solution. However, away from the optimal point in the parameter space,  $\tau$  is an important parameter in determining the model behavior.

*Bayesian sensitivity analysis:* BSA provides information how well the model parameters are constrained. For the case of *P. aeruginosa* (Fig 5), the parameters  $a_1$ ,  $a_2$ ,  $\delta$  and  $\tau$  are well-constrained and, therefore, sensitive model parameters. This is consistent with GSA, which is expected because both analyses are global in their nature. BSA also suggests correlation between estimates for  $a_2$  and  $\delta$ . The other model parameters are not correlated. The correlation is supported by the similarity in the time dependence of  $a_2$  and  $\delta$  sensitivities as shown in Figure 3b. Some of the parameters,  $a_1$ ,  $a_2$ , and  $\delta$ , have peaked posterior distributions, indicating a most probable value at the maximum. The parameter  $\tau$  is considered to be sensitive because the posterior range (from  $\sim 1.6$  to  $\sim 1.68$ ) is smaller than the prior range ( $0 - 4$ ; all the values are  $\log_{10}$  transformed and presented in Tables 2 and 3). However, the posterior distribution within this range is relatively flat (i.e. uniform). The flat distribution leads to a small sensitivity of the model to changes in this parameter using LSA.

# *Interpretation of predictions of permeability and efflux*

For *E. coli*, the values of the accumulation factor  $\phi > 1$  indicate trapping of antibiotic. The trapping is weak for  $t < \tau$  and becomes stronger at  $t = \tau$ . The greater magnitude of  $\alpha$  compared to  $\varepsilon$  values indicates that the permeability dominates the response. For *P. aeruginosa*, the values of  $\phi < 1$  indicate that efflux of antibiotic is important. For *S. aureus*, the value  $\phi > 1$  indicates a net trapping of antibiotic, like *E. coli*. In contrast to *E. coli*, the comparable magnitudes of  $\alpha$  and  $\varepsilon$  indicate that permeability and trapping are roughly equally important in during the whole time course.

The predictions suggest efflux is unimportant in the response of *E. coli* and *S. aureus* to ofloxacin. Permeation and trapping instead dominate the response. In contrast, efflux is predicted to be important in the response of *P. aeruginosa* to ofloxacin. The initial accumulation is less than what would be expected by permeation alone, indicating an efflux effect. In addition, the antibiotic level slowly decreases after the initial uptake, indicating an increase of efflux with time, presumably due to an adaptive response involving pump production.

The predictions for *E. coli* are especially intriguing. The response involves a  $\sim 50$ -fold decrease in permeability about 800 seconds after exposure, which would naively be expected to increase resistance [10]. However, the decrease in permeability is accompanied by a  $\sim 10$ -fold decrease in trapping. Because the decrease in trapping is less than the decrease in permeability, the result is an increase, rather than a decrease, in antibiotic accumulation.

Similar to the subtle connection found here between permeability and resistance, Nagano and Nikaido [5] used mathematical modeling to show how efflux pump deletion or overexpression might not change the MIC value of strong efflux pump substrates. It is interesting to consider these findings in light of a recent survey of physical properties of active compounds in a drug screening collection and their relation to whole cell antibacterial activity [20]. The survey reported on the difficulties encountered in simultaneously optimizing both biochemical potency and antibacterial activity, and concluded that “what is clearly needed is greater insight into medicinal chemistry strategies which optimize transport through porins and decrease efflux through the prolific efflux pumps.” Together, the findings reported here and elsewhere [5,6] suggest that mathematical modeling of permeation and efflux can be a key tool in enabling antibacterial medicinal chemistry.

Our results indicate that detailed, quantitative analysis of antibiotic accumulation time courses using mathematical modeling can yield new insights and experimentally testable predictions about mechanisms of drug resistance. The sensitivity analysis provides basis for distinguishing important from unimportant predictions. The predictions imply that decreasing permeability is not always an effective strategy for bacteria to increase drug resistance. This outcome in particular provides an example of the potential pitfalls involved in reasoning about structure-function relations in biochemical networks [21], and reinforces the need for incorporating mathematical modeling into strategies for fighting drug resistance.

Overall this study illustrates the key role that mathematical modeling and sensitivity analysis can play in deep interpretation of experimental data in biology.

## Materials and Methods

### *Model*

The time dependence of accumulated drug  $a(t)$  is modeled using

$$\frac{da(t)}{dt} = \alpha(t)a_o - \beta(t)a(t) \quad (1)$$

where  $a_o$  is the environmental antibiotic concentration,  $\alpha(t)$  is the specific import rate, and  $\beta(t)$  is the specific export rate. Here and elsewhere the terms “import” and “export” refer to combined effects of passive and active transport, and the term “specific” is sometimes used to indicate that the rate constant is multiplied by the antibiotic concentration. Both  $\alpha(t)$  and  $\beta(t)$  may change depending on the phase of the response. The import rate  $\alpha(t)$  is given by

$$\alpha(t) = \begin{cases} \alpha_1, & t < \tau \\ \alpha_2, & t \geq \tau \end{cases} \quad (2)$$

where  $\alpha_1$  applies to the initial phase of the accumulation dynamics ( $t < \tau$ ), and  $\alpha_2$  applies to the later phase ( $t \geq \tau$ ).

The export rate  $\beta(t)$  is given by

$$\beta(t) = \begin{cases} \beta_1, & t < \tau \\ \beta_2[1 + \delta(t - \tau)], & t \geq \tau \end{cases} \quad (3)$$

where  $\beta_1$  applies during the initial phase ( $t < \tau$ ),  $\beta_2$  applies during the later phase ( $t \geq \tau$ ), and  $\delta$  is the fractional rate of increase of export during the later phase.

Assuming  $\delta \ll \beta_2$  and  $\delta(t - \tau) \ll 1$  yields

$$a(t) = \begin{cases} e^{-\beta_1 t} a(0) + (1 - e^{-\beta_1 t}) a_1, & t \leq \tau \\ e^{-\beta_2(t-\tau)} a(\tau) + [1 - e^{-\beta_2(t-\tau)}] \frac{a_2}{1 + \delta(t - \tau)}, & t > \tau \end{cases} \quad (4)$$

where  $a_1 = \alpha_1 a_0 / \beta_1$ , and  $a_2 = \alpha_2 a_0 / \beta_2$ .

Given additional assumptions, the  $\alpha$  and  $\beta$  parameters can be used to derive permeation and efflux or trapping rates (see below). The  $\delta$  parameter models long-term adaptation by, e.g., gene regulation.

### ***Parameter estimation***

Parameter estimation for Eq. (4) was performed using published experimental time courses of ofloxacin accumulation in *E. coli*, *P. aeruginosa*, and *S. aureus* [7]. Data points were extracted from Figure 1 in Ref. [7]. Numerical solutions to Eq. (4) were obtained for each data point using functions defined in Mathematica Version 10 (Wolfram Research, Inc., Champaign, IL). As the estimated errors were the same for all data points [7], an unweighted mean squared deviation (MSD) between the model and the data was used as a target function for fitting. The MSD was minimized with respect to values of  $a_1$ ,  $a_2$ ,  $\beta_1$ ,  $\beta_2$ ,  $\delta$ , and  $\tau$  using the `FindMinimum` method, assuming  $a(0)=0$ . The values of  $a_1$ ,  $a_2$ ,  $\beta_1$ ,  $\beta_2$ ,  $\delta$  were varied over twelve decades. For *E. coli* and *P. aeruginosa*, the value of  $\tau$  was varied from 0-10,000 s (covering the full span of each 3,600 s time course) to seek an optimal solution. For *S. aureus*, optimization was performed for  $\tau = 10,000$  s. Mathematica workbooks and experimental data for all cases are available in a compressed archive in the Supporting Information.

### ***Sensitivity analysis methods***

All analyses were performed using the open source code Model-Analysis and Decision Support (MADS), developed at Los Alamos National Laboratory (<http://mads.lanl.gov>).

**Global Sensitivity Analysis (GSA):** For our analysis, we used the Sobol Monte Carlo algorithm [14]. The algorithm estimates the total and main effect for each model



parameter. The total effect is the total contribution to the output model variance to a given model parameter, including all the combined effects caused by its interactions with any other model parameter. The main effect measures the impact of varying a single model parameter by itself. The total and main effect can be very similar when the model parameters are independent. Sobol Monte Carlo algorithm was performed using about  $10^6$  independent model evaluations. Additional analyses (not presented) demonstrated that the number of model evaluations is sufficient to achieve converges for the estimate quantities.

*Local Sensitivity Analysis (LSA)*: We used a finite difference method requiring a limited number of model evaluations (equal to the number of unknown parameters). As a result, we obtain a gradient matrix  $\mathbf{J}$  (i.e. the Jacobian) with dimensions  $[m \times n]$  where  $m$  is the number of model parameters and  $n$  is the number of model inputs. Each component of the  $\mathbf{J}$  matrix represents the local sensitivity of each model parameter to each model output [17]. We analyze the covariance matrix  $\mathbf{C}$  of model parameters which is computed as  $\mathbf{C} = [\mathbf{J}^T \mathbf{J}]^{-1}$ . The covariance matrix is frequently analyzed using eigenanalysis where eigenvectors and eigenvalues of the covariance matrix are explored. How dominant (important) is each eigenvector depends on the respective eigenvalues; the smaller the eigenvalue, the higher the importance of the eigenvector. The components of each eigenvector represent the contributions of each model parameter to the simultaneous variation of multiple parameters: the larger the absolute value of the components, the larger the contribution. Model parameters with large contribution in dominant eigenvectors are important

(sensitive) model parameters. Model parameters with large contribution in non-dominant eigenvectors are also unimportant (insensitive) model parameters. If several model parameters have important contribution in a single eigenvector, these model parameters are correlated. If these contributions have the same sign, the correlation is positive. If these contributions have opposite signs, the correlation is negative.

*Bayesian Sensitivity Analysis (BSA)*: The BSA was performed using the Robust Adaptive Metropolis Markov Chain Monte Carlo algorithm [22]. To assess the sensitivity of the model parameters to the model outputs we compared the prior and the posterior pdf's of the model parameters (Table 2 and 3, respectively). High sensitivity parameters show a posterior pdf that is substantially narrower than the prior pdf.

### ***Prediction of permeability and efflux***

Estimation of the model parameters enables prediction of permeability and efflux rates. Given  $a_o$ , the specific import rates may be calculated as  $\alpha_1 = a_1 \beta_1 / a_o$ , and  $\alpha_2 = a_2 \beta_2 / a_o$ . Assuming the import is due to permeation,  $\alpha_1$  and  $\alpha_2$  are the permeabilities. Next, assume the specific export rate  $\beta(t)$  is a sum of contributions from permeability,  $\alpha(t)$  and other effects,  $\varepsilon(t)$ , leading to

$$\varepsilon(t) = \begin{cases} \beta_1 - \alpha_1, & t < \tau \\ \beta_2[1 + \delta(t - \tau)] - \alpha_2, & t \geq \tau \end{cases} \quad (5)$$

When  $\varepsilon(t) > 0$ , outward flow is enhanced compared to permeation, and  $\varepsilon(t)$  is associated with efflux. When  $\varepsilon(t) < 0$ , the outward flow is decreased compared to permeation, and  $\varepsilon(t)$  is associated with trapping. The accumulation factor  $\phi(t) = \alpha(t)/\beta(t)$  is used as a measure of the importance of efflux or trapping. It is given by

$$\phi(t) = \begin{cases} a_1/a_o, & t < \tau \\ a_2/a_o [1 + \delta(t - \tau)], & t \geq \tau \end{cases} \quad (6)$$

Eqs. (5) and (6) are only valid under the same assumptions as for Eq. (4).

Predictions of  $\varepsilon(t)$  are only meaningful using reliable estimates of both  $a_1$  and  $\beta_1$  for  $t < \tau$ , or both  $a_2$  and  $\beta_2$  for  $t \geq \tau$ . In contrast,  $\phi(t)$  can be predicted without estimates of  $\beta_1$  or  $\beta_2$ .

The predictions involve information about the environmental drug concentration and the conversion of estimates  $a_1$  and  $a_2$  from ng/mg dry weight units (Table 1) to mg/L units. The environmental ofloxacin concentration in the experiments was 10 mg/L [7]. To convert  $a_1$  and  $a_2$  to mg/L units, following Ref. [23], we used a buoyant density of 1.1 g/mL and a 31% dry weight for *E. coli*, a buoyant density of 1.2 g/mL and a 48% dry weight for *P. aeruginosa* (transferred from *P. putidae*), and assume a buoyant density of 1.1 g/mL and a 40% dry weight for *S. aureus*. This yielded

conversion factors of 0.341 mg dry weight/L for *E. coli*, 0.528 mg dry weight/L for *P. aeruginosa*, and 0.440 mg dry weight/L for *S. aureus*.

## Acknowledgments

This study was supported by the US Department of Energy under Contract DE-AC52-06NA25396 through the Laboratory-Directed Research and Development Program at Los Alamos National Laboratory under project number 20140121DR, Combating Antibiotic Resistance: Targeting Efflux Pump Systems at Multiple Scales.

## References

1. Li XZ, Nikaido H (2009) Efflux-mediated drug resistance in bacteria: an update. *Drugs* 69: 1555-1623.
2. Kourtesi C, Ball AR, Huang YY, Jachak SM, Vera DM, et al. (2013) Microbial efflux systems and inhibitors: approaches to drug discovery and the challenge of clinical implementation. *Open Microbiol J* 7: 34-52.
3. Nikaido H, Pages JM (2012) Broad-specificity efflux pumps and their role in multidrug resistance of Gram-negative bacteria. *FEMS Microbiol Rev* 36: 340-363.
4. Nikaido H, Normark S (1987) Sensitivity of *Escherichia coli* to various beta-lactams is determined by the interplay of outer membrane permeability and degradation by periplasmic beta-lactamases: a quantitative predictive treatment. *Mol Microbiol* 1: 29-36.
5. Nagano K, Nikaido H (2009) Kinetic behavior of the major multidrug efflux pump AcrB of *Escherichia coli*. *Proc Natl Acad Sci U S A* 106: 5854-5858.
6. Lim SP, Nikaido H (2010) Kinetic parameters of efflux of penicillins by the multidrug efflux transporter AcrAB-TolC of *Escherichia coli*. *Antimicrob Agents Chemother* 54: 1800-1806.
7. Asuquo AE, Piddock LJ (1993) Accumulation and killing kinetics of fifteen quinolones for *Escherichia coli*, *Staphylococcus aureus* and *Pseudomonas aeruginosa*. *J Antimicrob Chemother* 31: 865-880.

8. Diver JM, Piddock LJ, Wise R (1990) The accumulation of five quinolone  
antibacterial agents by *Escherichia coli*. *J Antimicrob Chemother* 25: 319-333.
9. Thanassi DG, Suh GS, Nikaido H (1995) Role of outer membrane barrier in efflux-  
mediated tetracycline resistance of *Escherichia coli*. *J Bacteriol* 177: 998-  
1007.
10. Schweizer HP (2012) Mechanisms of antibiotic resistance in *Burkholderia*  
*pseudomallei*: implications for treatment of melioidosis. *Future Microbiol* 7:  
1389-1399.
11. Sobol' IM (1990) On sensitivity estimation for nonlinear mathematical models.  
*Matematicheskoe Modelirovanie* 2: 112-118.
12. Sobol' IM (1993) Asymmetric convergence of approximations of the Monte Carlo  
method. *Computational mathematics and mathematical physics* 33: 1391-  
1396.
13. Saltelli A, Andres TH, Homma T (1993) Sensitivity Analysis of Model Output - an  
Investigation of New Techniques. *Computational Statistics & Data Analysis*  
15: 211-238.
14. Saltelli A, Ratto M, Andres T, Campolongo F, Cariboni J, et al. (2008) *Global*  
*Sensitivity Analysis: The Primer*: John Wiley & Sons.
15. Savageau MA (1976) *Biochemical systems analysis: a study of function and*  
*design in molecular biology*. Reading, MA: Addison-Wesley.
16. Savageau MA (2013) *System design principles*. In: Wall ME, editor. *Quantitative*  
*Biology: From Molecular to Cellular Systems*. Boca Raton: Taylor and Francis.  
pp. 23-49.
17. Gustafson P, Srinivasan C, Wasserman L (1995) Local sensitivity analysis.  
*Bayesian Statistics* 5: 631-640.
18. Oakley JE, O'Hagan A (2004) Probabilistic sensitivity analysis of complex  
models: a Bayesian approach. *J Roy Stat Soc B* 66: 751-769.
19. Weiss R (1996) An approach to Bayesian sensitivity analysis. *J Roy Stat Soc B* 58:  
739-750.
20. Brown DG, May-Dracka TL, Gagnon MM, Tommasi R (2014) Trends and  
exceptions of physical properties on antibacterial activity for Gram-positive  
and Gram-negative pathogens. *J Med Chem* 57: 10144-10161.
21. Wall ME (2011) Structure-function relations are subtle in genetic regulatory  
networks. *Math Biosci* 231: 61-68.
22. Vihola M (2012) Robust adaptive Metropolis algorithm with coerced acceptance  
rate. *Stat Comp* 22.
23. Bratbak G, Dundas I (1984) Bacterial dry matter content and biomass  
estimations. *Appl Environ Microbiol* 48: 755-757.

## Figures

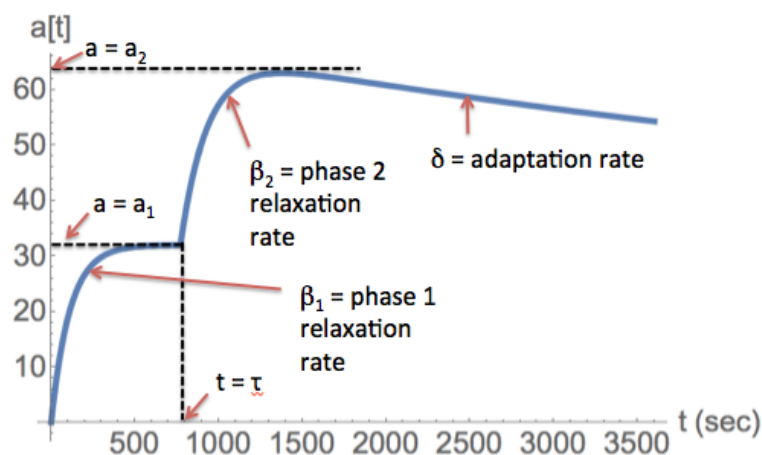


Figure 1. Behavior of the model and connection to model parameters.

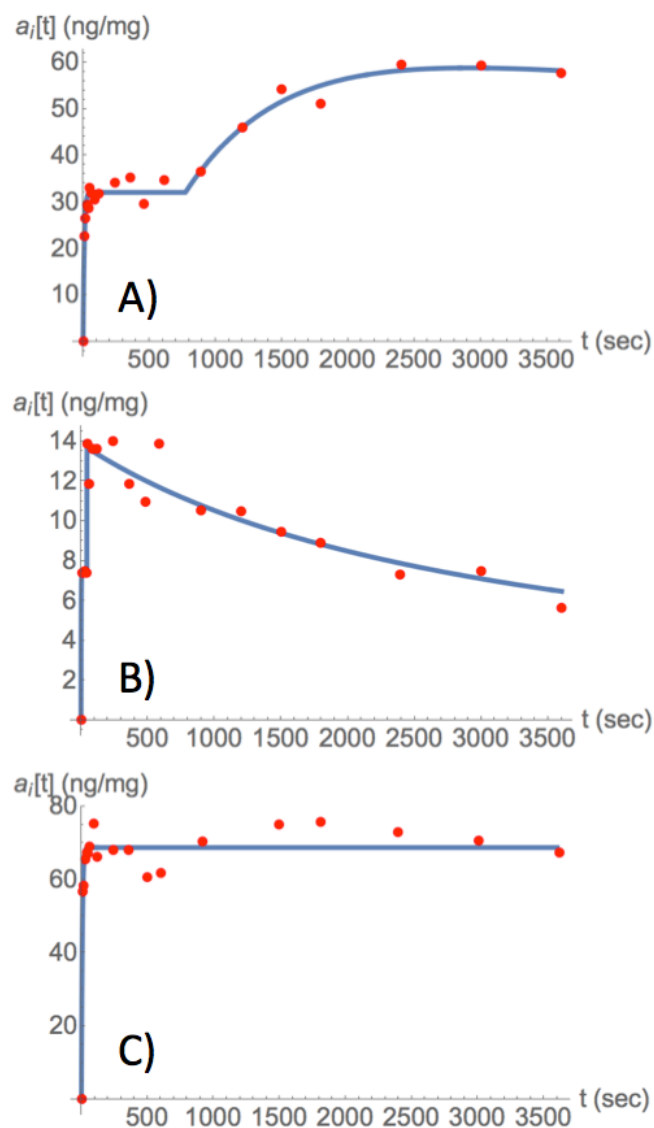
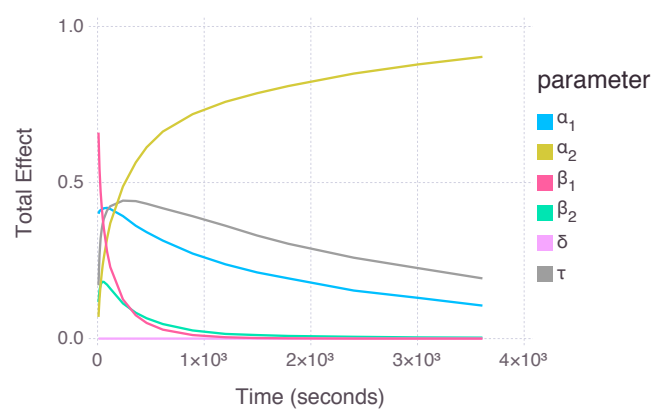


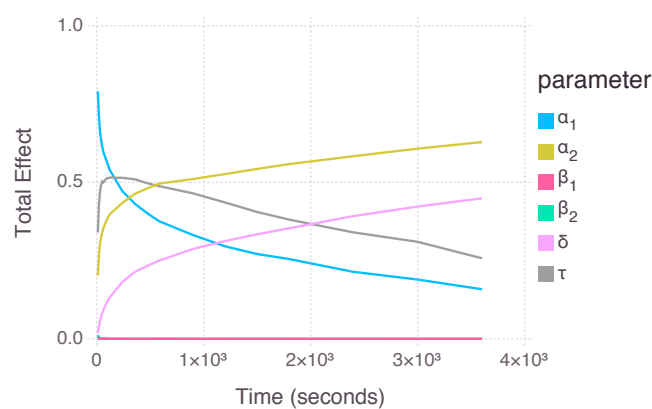
Figure 2. Fits of models to ofloxacin accumulation data. A) *E. coli*. B) *P. aeruginosa*. C) *S. aureus*. Following Ref. [7], the data are assumed to have a uniform measurement errors: 4.6 ng/mg for *E. coli*; 1.5 ng/mg for *P. aeruginosa*; and 8.7 ng/mg for *S. aureus*.

501 A)



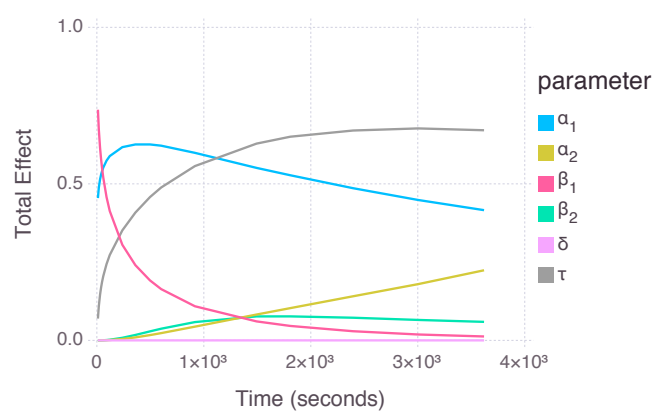
502

503 B)



504

505 C)



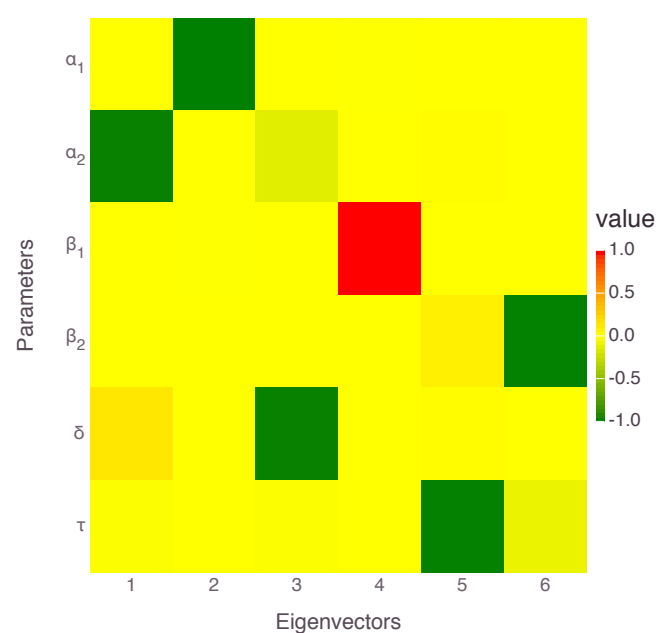
506

507



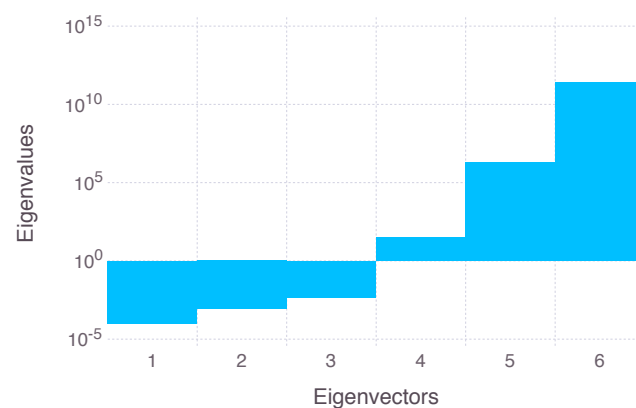
Figure 3. Global sensitivity of the model behavior to changes in parameter values for  
A) *E. coli*, B) *P. aeruginosa*, and C) *S. aureus* models. Sensitivity is quantified using  
the total effect measure in GSA. Color code:  $a_1$  (cyan);  $a_2$  (yellow);  $\beta_1$  (red);  $\beta_2$   
(green);  $\delta$  (pink); and  $\tau$  (grey).

515 A)



516

517 B)



518

519 Figure 4. Local sensitivity analysis for *P. aeruginosa*. (A) Eigenvector components  
520 associated with each model parameter. (B) Eigenvalues for each eigenvector,  
521 numbered in decreasing importance from left to right. The LSA identifies  $a_2$  as the  
522 most important model parameter because it contributes strongly to eigenvector 1,

523 and identifies  $\beta_2$  as the least important because it contributes strongly to  
524 eigenvector 6.

525

526

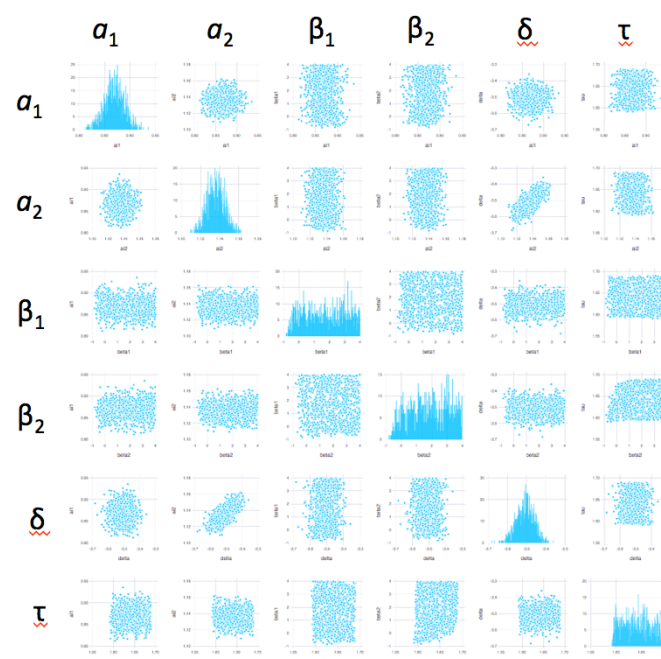


Figure 5. Bayesian sensitivity analysis for *P. aeruginosa*. The histograms along the diagonal represent the posterior pdf's of the model parameters constrained by the model observations. Off-diagonal subplots are scatter plots where each dot is a model-parameter set from the final MCMC sample. The horizontal axes define the parameter ranges (Table 3). The vertical axes along the diagonal plots define the frequency of occurrence. The vertical axes along the off-diagonal plots also define the parameter ranges (Table 3).

## Tables

Table 1. Estimated parameter values obtained after fitting the model to data on ofloxacin accumulation in different bacteria.

	$a_1$	$a_2$	$\beta_1$ (1/s)	$\beta_2$ (1/s)	$\delta$ (1/s)	$\tau$ (s)
	(ng/mg)	(ng/mg)				
<i>E. coli</i>	32.0	67.1	0.116	0.00125	(0.0000484)	772
<i>P. aeruginosa</i>	7.43	13.7	(0.682)	(3.01)	0.000314	44.5
<i>S. aureus</i>	68.71	(16.8)	0.149	(0.0119)	(0)	(10 <sup>4</sup> )

<sup>a</sup>Numbers in parentheses are unreliable according to the sensitivity analysis. They are included only for completeness.

Table 2. Prior parameter ranges ( $\log_{10}$  transformed values).

	$a_1$	$a_2$	$\beta_1$ (1/s)	$\beta_2$ (1/s)	$\delta$ (1/s)	$\tau$ (s)
	(ng/mg)	(ng/mg)				
min	0	0	-1	-1	-7	0
max	2	2	4	4	0	4

Table 3. Posterior parameter ranges based on Bayesian sensitivity analysis for *P*.

*aeruginosa* ( $\log_{10}$  transformed values).

	$a_1$	$a_2$	$\beta_1$ (1/s)	$\beta_2$ (1/s)	$\delta$ (1/s)	$\tau$ (s)
	(ng/mg)	(ng/mg)				
min	0.8	1.11	-1	-1	-3.65	1.6
max	0.92	1.16	4	4	-3.4	1.68

Table 4. Predicted accumulation factors ( $\phi$ ), permeabilities ( $\alpha$ ), and efflux ( $\epsilon > 0$ ) or trapping ( $\epsilon < 0$ ) rates.

	$\phi(t < \tau)$	$\phi(t = \tau)$	$\alpha_1$ (1/s)	$\alpha_2$ (1/s)	$\epsilon(t < \tau)$ (1/s)	$\epsilon(t = \tau)$ (1/s)
<i>E. coli</i>	1.09	2.29	0.13	0.0029	-0.011	-0.0016
<i>P. aeruginosa</i> <sup>a</sup>	0.39	0.72	(0.27)	(2.2)	(0.41)	(0.83)
<i>S. aureus</i> <sup>a</sup>	3.02	(0.74)	0.45	(0.01)	-0.30	(0.0031)

<sup>a</sup>Numbers in parentheses are unreliable according to the sensitivity analysis. They are included only for completeness.